2007 IEEE International Conference on
Robotics and Automation
Roma, Italy, 10-14 April 2007

A Physical Model and Control Strategy for Biped Running

Muhammad E. Abdallah
Robotic Locomotion Lab
Stanford University
Stanford, CA 94305
mesam@stanford.edu

Kenneth J. Waldron
Robotic Locomotion Lab
Stanford University
Stanford, CA 94305
kwaldron@stanford.edu

***Abstract*—We are in the process of building a biped robot capable of highly dynamic maneuvers. Implementing such maneuvers in real-time entails heuristic controllers founded on a grasp of the dynamics. We present here an analysis of the mechanics of biped running and a control strategy for stable running. By expounding on the direction of the ground-reaction forces and utilizing an impulse representation of the contact phase, we present a tractable model of the mechanics. This model motivates the control strategy and provides a basis for extending the strategy to more general systems. The control strategy consists of a simple set of three rules, where the key rule considers the leg-length upon liftoff. This rule offers a simple control for both steady-state and accelerated running. We present the *equilibrium running index* as a characterization of biped running. It relates the parameters affecting running and has broad applicability to biological and robotic systems. The control strategy was verified in simulation and the results are presented.**

I. Introduction

Raibert introduced his pioneering work in dynamic legged locomotion in the early 1980's with his series of hopping, telescoping legged robots [1]. He was able to achieve his breakthrough by way of a control strategy noteworthy for its simplicity; it controlled the forward velocity, hopping height, and body posture with simple, independent rules. This strategy was gleaned from the dynamics of the Spring Loaded Inverted Pendulum (SLIP) model that served as the basis for both his design and control. The SLIP model consists of a massless, spring-operated leg connected to the center of mass (CM) of the body. It has been widely utilized in the study of both biological and robotic systems [2]–[4]. Twenty years later, Raibert's robots still set the standard in dynamic motion for bipeds.

Others have also achieved running gaits in their robots. The trio of QRIO, ASIMO, and HRP, are the most advanced existing robots and have reported successful running [5], [6]. Their running stability, however, are all of the *ZMP-type* in which the center of pressure is maintained in the interior of the foot. In other words, they run with flat feet. Achieving a flight phase, a common definition for running, is possible with the ZMP criteria; however, the range of dynamics is constrained [7]. Fully dynamic motion cannot be constrained from gaining the unactuated degree of freedom represented by the foot tipping on a point or edge.

Two other robots and their strategies have targeted this fully-dynamic, underactuated running. The Iguana robot runs with sinusoidal inputs to the hip; however, it has effectively no body inertia thus allowing for such a simple controller [8]. Rabbit, on the other hand, is to our knowledge the only significant robot with articulated legs that has achieved fully dynamic running. Rabbit has point feet and implements a model-based hybrid controller [9].

The key to Raibert's success lies in his exploitation of the SLIP dynamics with his simple algorithm. A broader study of the mechanics of running offers the potential for a similarly simple strategy with wider applicability.

Our aim is to present a physical model of running and a simple control strategy that can allow for real-time, highly-dynamic motion on a real system unconstrained by the SLIP model. We are seeking a heuristic controller embodied in a set of simple rules that are inspired by the physics and exploit the dynamics of the system. The strategy should extend to a wider range of systems in which the legs are articulated, the CM does not coincide with the hip, and the actuation is varied.

We will investigate the mechanics of biped running independent of any control algorithm, and present principles and measures for equilibrium running. We then introduce a control strategy that achieves stable running. The system was studied extensively in simulation on a seven degree of freedom (DOF) planar model with telescoping legs. These results are presented here. It was further studied on a more general, articulated system with multiple actuation schemes—indicating its robustness and potential for physical implementation. This study is part of our on-going work to build a robotic biped that can implement highly-dynamic maneuvers.

II. The Dynamics of the GRF

The GRF for each leg upon impact is heavily influenced by the dynamics of the multi-body system. Determining an *a-priori* relation for the magnitude or direction of the GRF would offer a great tool for deriving a simplified control strategy. Fig. 1 shows the free-body diagram of the leg system upon impact.

The dynamic equation for the leg at impact follows. We assume that the ground contact is a point contact imparting

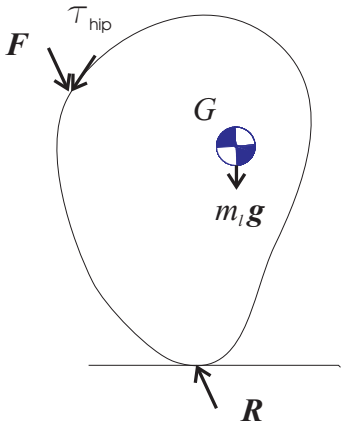

Fig. 1. The free-body diagram for a general leg system. External contact forces are applied at the hip and ground contact.

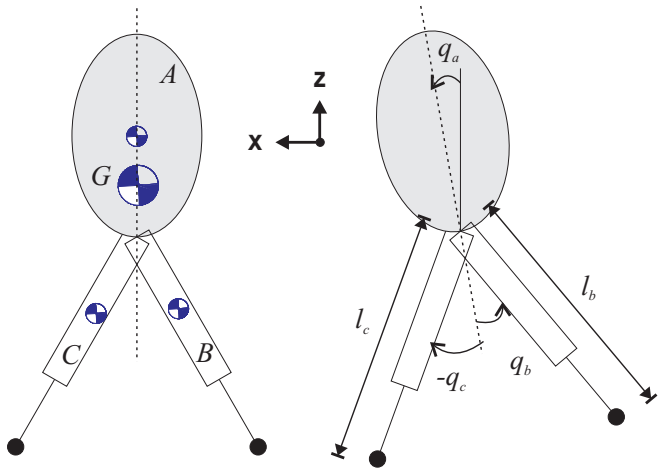

Fig. 2. The Biped Running Model is a simplified model of a general biped suited for running analysis. It is the simplest structure that still captures the mechanics of running for a general biped. The configuration variables are shown to the right. All positive angles are counter-clockwise.

no moments.

$$\boldsymbol{R} + \boldsymbol{F} = m_l \boldsymbol{a}_G - m_l \boldsymbol{g} \quad (1)$$

$$\boldsymbol{r}_{GR} \times \boldsymbol{R} + \boldsymbol{r}_{GF} \times \boldsymbol{F} = \tfrac{d}{dt}\boldsymbol{H}_G - \boldsymbol{\tau}_{hip} \quad (2)$$

$\boldsymbol{R}$ and $\boldsymbol{F}$ are the reaction forces at the ground and hip respectively. $\boldsymbol{\tau}_{hip}$ is the torque applied at the hip. m_l is the mass of the leg. $\boldsymbol{a}_G$ is the acceleration of the CM of the leg, G. $\boldsymbol{g}$ is the acceleration of gravity. $\boldsymbol{H}_G$ is the angular momentum about the CM. And the position vectors from G to the point of action of force i are represented by $\boldsymbol{r}_{Gi}$.

Often, researchers assume massless legs in the dynamic analysis of legged systems. The validity of this assumption is questionable, particularly in biped systems where each leg carries an even greater proportion of the total inertia. During impact in high-stress maneuvers, however, this assumption gains accuracy. Running is one such maneuver. At that instant, the impact forces become much greater than the inertia and gravity terms. If the hip torque is reduced, the leg system has the potential to approximate a static *two-force member*, where $\boldsymbol{R}$ and $\boldsymbol{F}$ become equal and opposite, and coaxial.

A human generates peak impact forces during running of 2-3 times the total body weight [10]–[12], and robotic systems generate forces around 3-5 times the body weight [13]. Using anthropomorphic proportions, the total mass is about six times the mass of one leg. This indicates an impact force around 20 times greater than the gravitational force. Similarly, even if the leg acceleration reaches values as high as $2g$, the inertial force would still be 10 times less than the impact force. We can thus expect the net gravitational and inertial forces to represent merely 5-10% of the impact force.

Under such conditions, we can safely neglect the inertia, gravity, and torque terms—approximating a static two-force member. Hence, *the ground reaction force $\boldsymbol{R}$ acts principally along the axis of the leg*.

This assumption will prove very useful in designing a control strategy to achieve running. Data on animal running supports this assertion and has been displayed on a wide variety of animals from bipeds to quadrapeds and even hexapeds [14]–[17]. Although this behavior has been well known in animals, its source has not been understood or addressed [4]. We show here that it is dominated by the inherent dynamics of the system rather than active control.

This behavior can be employed in a robotic system by recognizing the following principles. First, it is primarily a product of the dynamics of running. Second, it can be enhanced by both reducing the hip torques and restraining the internal motion of the leg.

III. The Biped Running Model

Based on this assumption of axial thrusts, we will work with a simplified model of a biped with telescoping legs. The analysis of the previous section characterizes the external physics of the leg. Thus, we will deal with this two DOF *virtual leg* in lieu of a general articulated system to simplify the internal kinematics and dynamics of the leg.

We will refer to this model as the *Biped Running Model*, shown in Fig. 2. It consists of three rigid bodies, representing the torso and two legs, connected by a revolute joint at the hip. The CM's of the bodies are at fixed displacements from the hip. The feet are point-masses connected by prismatic joints to the legs. G represents the CM of the entire system.

We will assume the leg DOF are fully active, and thus R can be arbitrarily set. We assume that the GRF profile is symmetric about the middle of the stance. In this study here, we will chose to apply a constant magnitude R.

Actuating the desired R in this model is quite simple; it becomes more of a challenge in an articulated system. The desired R will be actuated by setting the prismatic actuator force of the contact leg equal to R. This is a good approximation since the unsprung mass that is the foot is negligible.

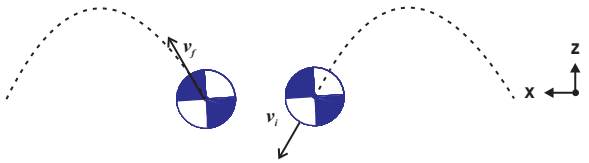

Fig. 3. Steady-state running has the CM mirror a conservative ball which rebounds from the ground impact with the linear momentum reflected about the horizontal.

IV. Steady-State Running

Equilibrium here is achieved over the cycle of a single step. Each step includes a contact phase and the subsequent flight phase.

We will control the global CM of the system, G, using the impulse-momentum relationship. The two legs are maintained in opposition during both the contact and flight phases. This counters the pitch moments during swinging. It also stabilizes the position of G. With this rule, G will be approximately fixed in position relative to the bodies; it will shift only slightly up and down the center line.

The external impulse needed to maintain the periodic motion and counter the vertical impulse of gravity can only be applied during the contact phase. If the biped enters the contact phase with a CM velocity $\boldsymbol{v}_i$, then steady-state is maintained by:

1) Keeping the horizontal velocity constant ($v_{xf} = v_{xi}$).
2) Reversing the vertical velocity ($v_{zf} = -v_{zi}$).

This is akin to a ball bouncing conservatively as shown in Fig. 3. The subscript i refers to the initial instant of ground contact, i.e. touchdown. The subscript f refers to the final instant of contact, i.e. liftoff. Note that we are not modelling the system as a lumped-mass; rather, we are considering the CM and regulating its relative position using the internal configuration of the system.

If $\boldsymbol{i_R}$ is the net impulse from $\boldsymbol{R}$ over the contact phase, the desired net impulse at each stance is,

$$i_{Rx} = 0 \tag{3}$$

$$i_{Rz} = 2mv_{zi}. \tag{4}$$

The subscripts x and z represent the horizontal and vertical components respectively.

Given a profile for $\boldsymbol{R}$, a solution can be found for the initial and final angle needed to achieve the desired impulse $\boldsymbol{i_R}$. The assumption that R will be actuated as a constant has already been stated. The next step is to determine its magnitude.

We will now propose a control strategy to achieve steady-state, constant velocity running. The equilibrium state produced by this strategy will be analyzed. Then we will turn to the strategy for accelerated running.

V. The Control Strategy

The proposed control strategy for the contact phase consists of the following three rules.

1) Maintain an upright torso: $q_a = 0$.

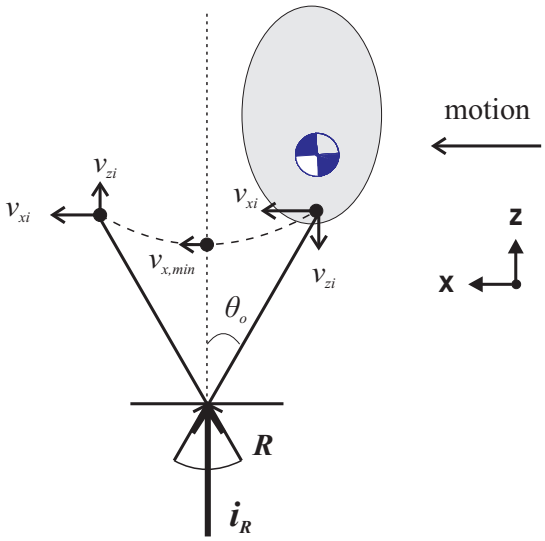

Fig. 4. Equilibrium running results in a symmetric condition for the contact phase. The symmetry is reflected in the velocities, configuration, and contact forces. The velocity of the hip is approximately equal to the velocity of the CM during contact since the torso motion is regulated. The CM shown here is for the entire system (G).

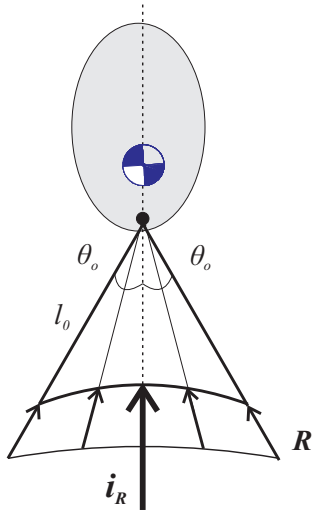

Fig. 5. The symmetric contact for equilibrium running is shown here in the body reference frame. The distribution of contact forces results in a net impulse that is vertical and points through the global CM. In this paper, we will be actuating a constant ground reaction force.

2) Operate the swing leg in opposition to the contact leg: $q_c = -q_b$.
3) Sweep the contact leg through an equal leg-length: $l_{bf} = l_{bi}$.

Rule 3 entails measuring the leg-length upon touchdown and releasing from the ground once the length reaches that initial, touchdown length. This rule is the key to the stability of the system. At equilibrium running, this strategy will produce a symmetrical condition for the contact phase.

Under the right conditions, the leg will reach the initial length at an equal angle to the initial angle, sweeping a symmetrical range of $2\theta_o$. The angle of the leg with respect to

the vertical is represented by θ, and θ_o is the initial angle. Fig. 4 shows this equilibrium state and its symmetry. G is shown lying on the line of symmetry of the biped. The leg starts at the length l_o and releases when the length reaches l_o again.

This strategy aims to create a vertical impulse that points through G. Fig. 5 shows the distribution of the forces over the contact phase in the reference frame of the body. The strategy regulates G by holding it vertically above the hip. It then swings the leg through a symmetrical span to create a vertical net impulse pointing through the hip and hence G.

As a result of the symmetry, the resultant impulse $\boldsymbol{i_R}$ is purely vertical. The constant magnitude of $\boldsymbol{R}$ can then be set to achieve the desired vertical impulse. The next section derives a relation that solves for this desired magnitude.

The result here bears a resemblance to Raibert's strategy and his utilization of symmetry and the neutral point. The difference is that this strategy is based on an analysis of the external forces and CM motion, rather than the SLIP model. This impulse-momentum analysis offers it the potential for wider applicability.

VI. The Equilibrium Running Index (ERI)

A. Derivation of the Index

We will now solve for the value of R needed for this equilibrium state. First, we will determine the contact time by considering the vertical motion. The force-balance equation for the vertical direction is,

$$R\cos(\theta) - mg = ma_z \tag{5}$$

where a_z is the vertical acceleration of G.

The leg will reach angles θ of at most $20^\circ - 30^\circ$ during running, making the assumption of a constant vertical acceleration valid. Let $\cos(\theta) = 1$, introducing average errors of less than 5%. The resulting acceleration is,

$$a_z = \frac{R}{m} - g. \tag{6}$$

The vertical velocity starts at v_{zi} and reverses direction at the endpoint as shown in Fig. 4. Since a constant acceleration has been assumed, the contact time t_c can be determined as follows.

$$\begin{aligned} t_c &= \frac{2v_{zi}}{a_z} \\ t_c &= \frac{2mv_{zi}}{R - mg} \end{aligned} \tag{7}$$

Now we will solve for the same contact time considering the horizontal motion instead. The horizontal velocity v_x follows a periodic curve with only minor deviations from its mean. Remaining constant during flight, the speed drops slightly during contact only to return to the same initial value. The velocity v_x can thus be replaced safely with its average, ηv_{xi}. η is a positive constant of slight variation across conditions; it can be shown that a good approximation is $\eta = 0.9$.

The vertical distance covered is $2l_o\sin(\theta_o)$, resulting in a contact time of,

$$t_c = \frac{2l_o\sin(\theta_o)}{\eta v_{xi}}. \tag{8}$$

Solving for (7) and (8) produces the following equilibrium relationship between the GRF, the leg-angle, and the touchdown velocities of the CM.

$$(R - mg)\ l_o\sin(\theta_o) = \eta m v_{xi} v_{zi} \tag{9}$$

The relation can be simplified with the small-angle approximation, $\sin(\theta_o) = \theta_o$. This introduces errors of less than 5% for the angles of interest.

$$l_o\theta_o\ (R - mg) = \eta m v_{xi} v_{zi} \tag{10}$$

We will now define the **equilibrium running index**, e, as a measure of this equilibrium condition.

$$e = \eta\frac{m v_{xi} v_{zi}}{l_o\theta_o\ (R - mg)} \tag{11}$$

A measure of $e = 1$ indicates the equilibrium state. It will prove to be a great tool for characterizing the running behavior, studying the stability of the gait, and deriving design criteria for running performance.

Koechling follows a similar analysis to reach (7) and (8) [18]. He does not, however, combine them for a single measure as shown here.

B. Relevance of the Index

The ERI is essentially a ratio of the contact times in the horizontal and vertical directions when symmetry is fulfilled. It expresses the parameters and their dependencies for maintaining equilibrium. For example, if you wish to run at a higher speed v_{xi}, you will need to increase the impact force R, open the leg wider with θ_o, or increase the leg-length l_o.

The equilibrium index has wider applicability. Specifically, it applies to all systems with similar symmetry in the contact phase, such as spring-loaded systems. More generally, it applies to all ballistic legged-systems that model the conservative bounce of Fig. 3. In the general case, R represents the average GRF and the index is less numerically accurate; however, the parameters and their functionality as expressed are still valid.

This result is verifed in both biological and robotic systems, where the index consistently predicts the parameters and rules for running. It has been shown in many animals, including humans, that they accommodate higher speeds (v_x) by increasing their leg angles (θ_o) [3], [19]. Farley shows that when humans run with a constant forward velocity, a decrease in leg-stiffness (which translates into R) necessitates an increase in leg-angle (θ_o) [12]. Weyand, et. al show that at higher speeds (v_x), running humans need to increase their GRF [11]. Fig. 6 displays some of these behaviors in biological running.

McMahon and Cheng conducted numerical studies of the SLIP model for running and verified their results in biological systems [3]. They found that the peak GRF is proportional to both the forward velocity (v_{xi}) and the vertical velocity (v_{zi}). They also found that the peak GRF is inversely proportional

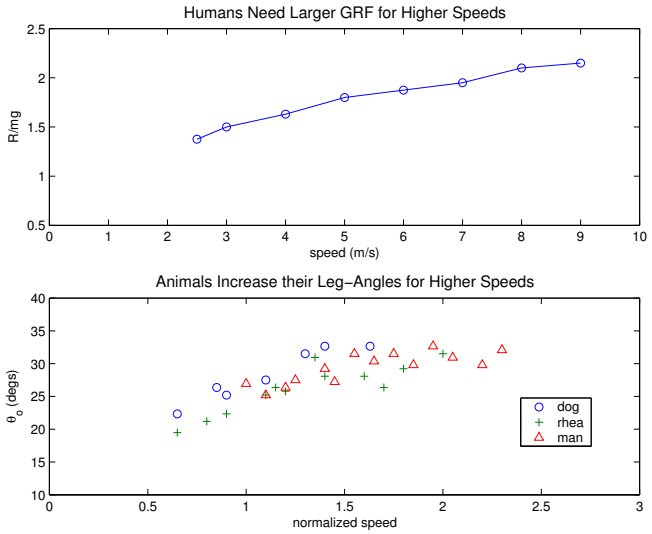

Fig. 6. Animal running behavior is consistent with the equilibrium index. In the first plot, Weyand, et. al analyze human running and plot the average GRF for various speeds [11]. They show that the average GRF grows in direct proportion to speed. In the second plot, McMahon and Cheng analyze multiple biological runners [3]. They show that the runners increase their leg-angles to accommodate higher speeds.

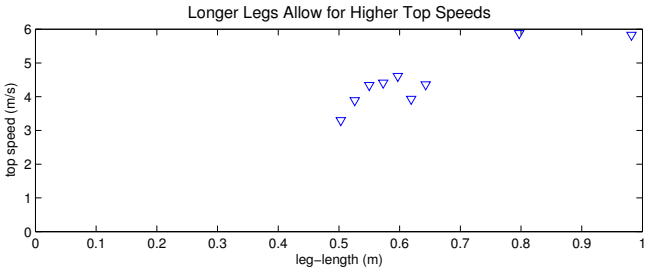

Fig. 7. Koechling tested his planar biped robot with various leg-lengths [18]. He demonstrated that longer legs allowed the robot to reach higher top speeds while still maintaining stability. This result is predicted by the equilibrium index.

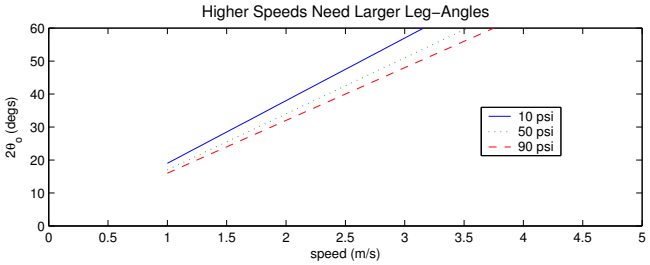

Fig. 8. Koechling increased the speed of his biped robot while maintaining a constant air-pressure in the pneumatic, telescoping leg [18]. The experiments were conducted at three different air-pressures. Greater air-pressures translate directly into greater GRF's. Shown here are the best least-squares fit to the data. This data verifies two results predicted by the equilibrium index. First, when R is constant, greater leg-angles are needed for higher speeds. Second, at a constant speed, increasing the GRF necessitates decreasing the leg-angle.

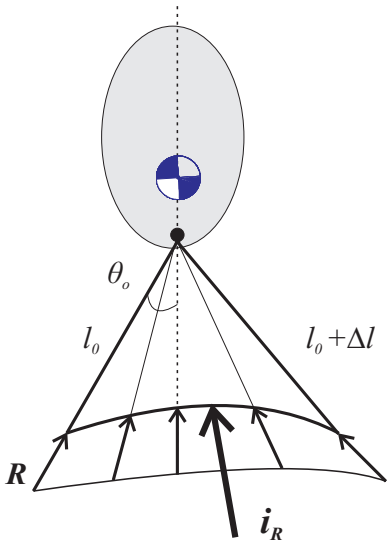

Fig. 9. The results of the accelerated control strategy are shown here. The release leg-length is extended to produce a net impulse with a forward component to provide the desired acceleration. The GRF's are shown here in the body reference frame.

to the leg-angle, and that the vertical and horizontal velocities are inversely proportional to each other.

Koechling and Raibert exhibited many of these relations on their running biped [18]. They showed that the top speed of their robot can be increased by increasing the leg-length (l_o), increasing the leg-stiffness (R), or increasing the leg-angle (θ_o). Figures 7 and 8 display some of these results.

All of these parameters and rules for biped running are predicted by the ERI. This is the strength of the measure. It combines these parameters and their interdependencies and expresses it in a simple relation.

C. *Stability of the System*

The gait exhibits a dynamic stability where the system converges to the equilibrium state as determined by the ERI. This stability covers a considerable range of dynamics and is limited primarily by extraneous factors. It can be shown that the stable region about equilibrium is limited not by the inherent dynamics and control strategy, but by the ground clearance and swing frequency of the non-support leg. This result was verified in simulation, and the system was shown to converge to equilibrium within an impressive range of 25% change in R.

VII. The Strategy for Accelerated Running

We will now consider the control strategy to produce a net forward thrust in the contact phase. This need arises in many situations, particularly when a change in speed is desired. Other instances include when the robot faces drag, uphill running, or running on soft terrain [20].

In this case, we want the contact leg to sweep an asymmetric angle that extends further back. This would produce a positive forward component in the net impulse as shown in Fig. 9.

The main mechanism for inducing this asymmetry will be the control of the release leg-length. To accelerate, we will allow the leg to reach a longer final length (compared to the initial length l_o). This extended contact results in a positive

TABLE I
MODEL PARAMETERS

	distance from hip to CM (m)	mass (kg)	inertia (kg m^2)
torso	0.34	48.3	8.12
leg	0.384	11.5	1.03
foot	0.8 (nominal)	1.0	0

forward component in the ground impulse. To decelerate we would invoke the opposite pattern, releasing at a shorter length.

The control strategy for acceleration employs the same rules as steady-state running, with the exception of the change to the final leg-length. The rules follow.

1) Maintain an upright torso: $q_a = 0$.
2) Operate the swing leg in opposition to the contact leg: $q_c = -q_b$.
3) Sweep the contact leg through an extended leg-length: $l_{bf} = l_{bi} + \Delta l$.

The leg-extension Δl offers a mechanism for accelerating and decelerating. It also offers a mechanism for error handling. Our assumptions of the negligible leg inertia and negligible hip torques introduce errors in the direction of the GRF. It is usually easy to introduce a slight leg-extension Δl that counters the errors and achieves equilibrium. In our simulation runs, any small Δl of around 1 cm was sufficient to allow the system to achieve steady-state running (compared to a leg length of 80 cm).

VIII. SIMULATION RESULTS

A. Dynamic Model

A fully dynamic simulation of the Biped Running Model shown in Fig. 2 was created. The foot-ground contact was modelled as a rigid, inelastic contact using motion constraints. Friction was assumed sufficient to avoid slip. The equations of motion were generated in Autolev^{TM}, a symbolic manipulator for dynamics applications [21]. A C program was developed to determine the appropriate constraint equations, solve for the equations of motion, and perform the integration using a variable-step integrator. The subsequent results were animated in an OpenGL interface. The biped modelled an average human being with the parameters shown in Table I.

B. Steady-state Run

The control strategy presented here for steady-state running was applied to the model. The model was released with a forward velocity of 3 m/s as an initial condition. During the contact phase, a constant force of 1400 N was applied to the prismatic actuator of the contact leg. With relative ease, the system succesfully achieved a stable running gait as shown in Fig. 10. After slight transience, the gait settled at equilibrium with a forward velocity of 3 m/s. Fig. 11 contains plots of the CM velocity and the ERI, displaying the periodic, equilibrium motion. The ERI was calculated using a factor of $\eta = 93\%$.

This simulation was actually run with a leg-extension of $\Delta l = 1$ cm. It turned out that with no leg-extension the biped slowed down over time. The leg-extension rule can thus be utilized to compensate for errors in the model approximations and actuation.

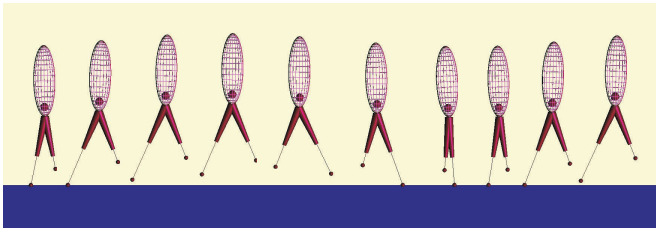

Fig. 10. The control strategy was successfully implemented on the Biped Running Model to produce a steady-state run of 3 m/s with a stable gait. Snapshots of the simulation are shown here. The sphere in the lower torso represents the CM of the system (G).

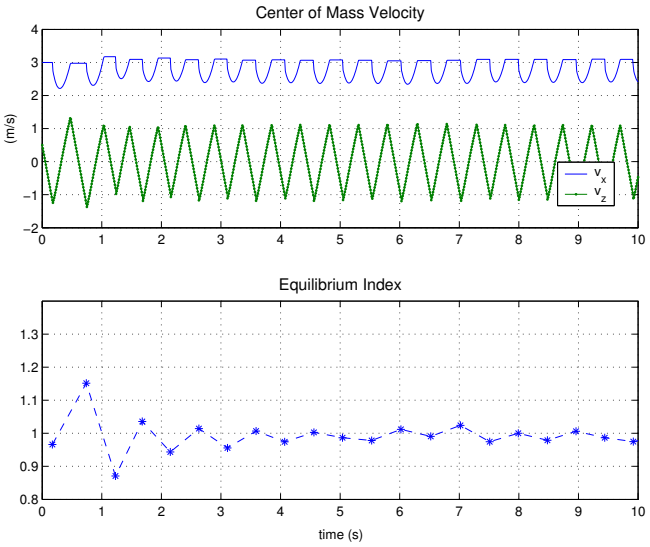

Fig. 11. Plots for the steady-state run shown in Fig. 10. The gait settled down at the steady-state velocity after some transience. The valleys in the horizontal velocity v_x represent the contact phase.

Fig. 12 shows plots of the GRF direction. The direction of the GRF closely follows the leg-angle, displaying the accuracy of the axial thrusts assumption.

C. Accelerated Run

The control strategy for accelerated running was then applied to the robot to accelerate it from 3 to 4 m/s. At 4

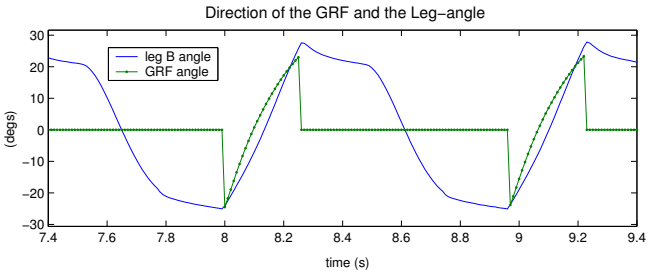

Fig. 12. The direction of the ground-reaction forces on leg B are shown for the constant 3 m/s run. Note the accuracy of the axial thrusts assumption.

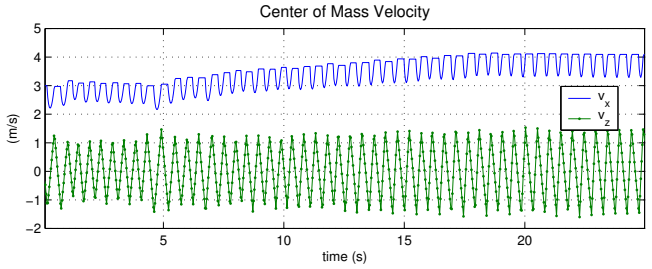

Fig. 13. The control strategy for accelerating was applied to accelerate the biped from 3-4 m/s. The leg-extension parameter was increased at 4s and then reduced again at 18s. Note the robot accelerating in that range and then settling at the new steady-state speed.

seconds into the run, the leg-extension was increased from 1 to 2 cm. At 18 seconds, the leg-extension was dropped to 1.5 cm, and the system settled into equilibrium. As the speed increased, we found it necessary to increase the actuated force correspondingly. This is predicted by the equilibrium index, where higher speeds require a higher GRF to maintain equilibrium. Every 2s, the actuated force was increased by 5%. Fig. 13 shows the system accelerating during that time range.

D. Beyond the Current Model

The strategy was further implemented with multiple actuation schemes on a higher DOF, articulated model. The schemes produced very different GRF profiles and some included passive elements. The variations were easily accommodated with simple, intuitive changes to physical parameters—parameters such as the desired torso pitch and the leg-extension.

These results offer promising conclusions for the physical implementation of the strategy. First, they indicate the robustness of the algorithm to the GRF actuation. Second, they demonstrate the flexibility for diverse actuation designs.

IX. Conclusion

We have presented a heuristic control strategy that achieves stable biped running. The strength of this strategy lies in its simplicity, with three basic rules that exploit the system dynamics.

The mechanics model underlying the strategy provides it with a basis for a broader applicability to bipeds. The physical model is highlighted by two features that lend this extendability. First, it deals with the actual CM of the system, regulating its relative position using the internal posture. Hence, it does not place limiting assumptions on the structure or mass distribution of the body. Second, it abstracts the GRF's with physical principles and an impulse-based representation that facilitates the accommodation of variance.

The model gives rise to the equilibrium running index, providing an elegant tool for the analysis, design, and control of biped runners. The index expresses the parameters effecting running and their functionality, and carries relevence to both biological and robotic bipeds.

In this paper, the strategy was applied to a telescoping legged system. In upcoming work, we apply it to an articulated system and discuss the issues presented by the articulation.

Acknowledgment

The authors wish to acknowledge the financial support of the National Science Foundation, grant number IIS-0535226 during the course of this work, and a fellowship from the ARCS Foundation held by Mr. Abdallah.

References

[1] M. Raibert, *Legged Robots that Balance*. Cambridge, MA: MIT Press, 1986.
[2] R. Blickhan, "The spring-mass model for running and hopping," *Journal of Biomechanics*, vol. 22, pp. 1217–1222, 1989.
[3] T. A. McMahon and G. C. Cheng, "The mechanics of running: How does stiffness couple with speed?" *Journal of Biomechanics*, vol. 23, no. Suppl. 1, pp. 65–78, 1990.
[4] W. Schwind, "Spring loaded inverted pendulum running: a plant model," Ph.D. dissertation, University of Michigan, 1998.
[5] K. Nagasaka, Y. Kuroki, S. Suzuki, Y. Itoh, and J. Yamaguchi, "Integrated motion control for walking, jumping, and running on a small bipedal entertainment robot," in *IEEE International Conference on Robotics and Automation*, New Orleans, LA, April 2004.
[6] S. Kajita, T. Nagasaki, K. Yokoi, K. Kaneko, and K. Tanie, "Running pattern generation for a humanoid robot," in *IEEE International Conference on Robotics and Automation*, Washington, DC, May 2002.
[7] C. Chevallereau, G. Abba, Y. Aoustin, F. Plestan, E. Westervelt, C. C. de Wit, and J. Grizzle, "Rabbit: A testbed for advanced control theory," *IEEE Control Systems Magazine*, pp. 57–79, October 2003.
[8] M. Lewis and L. Simo, "Certain principles of biomorphic robots," *Autonomous Robots*, vol. 11, pp. 221–226, 2001.
[9] C. Chevallereau, E. Westervelt, and J. Grizzle, "Asymptotically stable running for a five-link, four-actuator, planar bipedal robot," *International Journal of Robotic Research*, vol. 24, no. 6, pp. 431–464, June 2005.
[10] J. R. Hutchinson, "Biomechanical modeling and sensitivity analysis of bipedal running ability. i. extant taxa," *Journal of Morphology*, vol. 262, pp. 421–440, 2004.
[11] P. G. Weyand, D. B. Sternlight, M. J. Bellizzi, and S. Wright, "Faster top running speeds are achieved with greater ground forces not more rapid leg movements," *Journal of Applied Physiology*, vol. 89, pp. 1991–1999, 2000.
[12] C. T. Farley and O. Gonzalez, "Leg stiffness and stride frequency in human running," *Journal of Biomechanics*, vol. 29, no. 2, pp. 181–186, 1996.
[13] S. P. Singh, "Self-contained measurement of dynamic legged locomotion: Design for robot and field environments," Ph.D. dissertation, Stanford University, March 2006.
[14] R. M. Alexander, "Mechanics and scaling of terrestrial locomotion," in *Scale Effects in Animal Locomotion*, T. J. Pedley, Ed. London: Academic Press, 1977, ch. 6, pp. 93–110.
[15] A. A. Biewener, "Locomotory stresses in the limb bones of two small mammals: the ground squirrel and chipmunk," *Journal of Experimental Biology*, vol. 103, pp. 131–154, 1983.
[16] R. J. Full, R. Blickhan, and L. H. Ting, "Leg design in hexapedal runners," *Journal of Experimental Biology*, vol. 158, pp. 369–390, 1991.
[17] A. A. Biewener, *Animal Locomotion*. Oxford: Oxford University Press, 2003.
[18] J. Koechling, "The limits of running speed: Experiments with a legged robot," Ph.D. dissertation, Carnegie Mellon University, 1989.
[19] C. T. Farley, J. Glasheen, and T. A. McMahon, "Running springs: speed and animal size," *Jounral of Experimental Biology*, vol. 185, pp. 71–86, 1993.
[20] J. P. Schmiedler and K. J. Waldron, "The mechanics of quadrupedal galloping and the future of legged vehicles," *International Journal of Robotics Research*, vol. 18, no. 12, pp. 1224–1234, December 1999.
[21] T. R. Kane and D. A. Levenson, *Dynamics Online: Theory and Implementation with AUTOLEV*. Sunnyvale, CA: Online Dynamics, Inc., 1996.